Quantitative MHC class-I/-II gene expression levels in *CDK12* mutated prostate cancer reveal intratumorally T cell adaptive immune response in tumors

William Lautert-Dutra[1], Camila M. Melo[1], Luiz P. Chaves[1], Rodolfo B. dos Reis[1, 2], Sandro L. Bonatto[3] and Jeremy A. Squire[1, 4, *]

[1] Department of Genetics, Medicine School of Ribeirao Preto, University of São Paulo, Ribeirao Preto 14048-900, SP, Brazil.

[2] Division of Urology, Department of Surgery and Anatomy, Medicine School of Ribeirao Preto, University of São Paulo, Ribeirao Preto 14048-900, SP, Brazil.

[3] Escola de Ciências da Saúde e da Vida, Pontifícia Universidade Católica do Rio Grande do Sul, Av. Ipiranga, 668, 90619-900, Porto Alegre, RS, Brazil

[4] Department of Pathology and Molecular Medicine, Queen's University, Kingston, ON K7L3N6, Canada.

*Corresponding author: Department of Genetics, Medicine School of Ribeirao Preto, University of São Paulo, Ribeirao Preto 14048-900, SP, Brazil. Tel.: + 55 16 3602-3252; E-mail: squirej@fmrp.usp.br.

Abstract

Background: The inactivation of Cyclin-dependent Kinase 12, *CDK12*, has been used as a predictive biomarker of treatment response to immune-checkpoint blockade (ICB) in advanced prostate cancer (PCa). However, some patients with CDK12 alterations fail to respond to ICB. Changes in MHC expression have been linked to tumor progression and reduced response to ICB in different malignancies. **Methods:** Using transcriptome and WES data from primary (*n*=48) and metastatic (*n*=10) *CDK12* defective PCa; we investigated variation in the expression of the MHC genes and associated downstream changes. We divided the tumors into "High" and "Low" expression levels of MHC-I and -II based on gene expression quartiles. **Results:** *CDK12* defective tumors with increased MHC levels showed the activation of several pathways associated with the immune system and elevated *PD-L1*, *IDO1*, and *TIM3* expression. There was also increased composition of CD8+ T cells, B cells, γδ T cells, and M1 Macrophages in *CDK12* mutated tumors with elevated MHC levels. In contrast, *CDK12* defective tumors with decreased MHC expression were often subject to loss of heterozygosity (LOH) genomic events affecting MHC-I/-II and the *HLA* gene cluster on chromosome 6. **Conclusions:** Our data suggest that *CDK12* defective PCa express higher levels of classical MHC and have an active and inflamed tumor microenvironment with elevated immunomodulatory pathway expression and increased presence of effector T cells. The finding of lower MHC expression in tumors with LOH of associated genes on chromosome 6 suggests reduced MHC expression may be caused by acquisition of specific somatic genomic events that reduce the expression of these antigen presentation genes. Collectively, these data indicate that implementing a combined measure of *CDK12* mutation and MHC expression levels together with an evaluation of LOH status may better predict outcomes for prostate cancer tumors classified as eligible for ICB treatment.

Keywords: Biomarkers, Immunotherapy, Transcriptomics, TCGA, SU2C, Digital cytometry, Antigen Presentation, Immune evasion, Adaptive immune system, Loss-of-Heterozygosity (LOH)

Introduction

Treatment of advanced prostate cancer (PCa) remains a therapeutic challenge. Men with distant metastases at diagnosis have the worst overall survival (OS), with only 30% of patients surviving > 5 years [1]. For recurrent disease, acquired resistance to androgen deprivation therapy (ADT) and chemotherapy remains a significant cause of death [2]. Immune-checkpoint blockade (ICB) therapies, such as PD-L1 inhibition, have shown only significant benefits in a minority of patients [3]. Thus, it is necessary to discover and characterize the genetic pathways and molecular signatures that could help predict more effective disease progression control in advanced PCa.

The tumor mutation burden affects the infiltration of immune cells in the tumor microenvironment (TME) [4]. Because of the high load of neoantigens, tumors with defective DNA damage repair (DDR) pathways are more suitable for immunotherapy [5]. The biallelic inactivation of Cyclin-dependent Kinase 12, *CDK12*, was recently described as a novel immune active class of advanced PCa with a more aggressive phenotype, a high mutation burden derived from focal tandem duplication events, and high inflammatory and immune cell infiltrate distinct from other defective molecular subtypes [6]–[9]. Although this new subtype has been proposed as a predictive biomarker of treatment response to immune-checkpoint blockade (ICB) in advanced prostate cancer (PCa), many patients with *CDK12* alterations still fail to respond to ICB treatment. In a retrospective multi-center study, Antonarakis *et al.* found that just 33% of the *CDK12*-altered advanced PCa patients had a prostate-specific antigen (PSA) response and an increased progression-free survival of 5.4 months when treated

with anti-PD-1 therapy [10]. In another study, Schweizer *et al.* showed that of the nineteen advanced patients who received ICB, eleven (59%) showed a response based on a decline in PSA, with two patients (11%) having a 100% PSA decline. However, the molecular causes of ICB resistance in this molecular subtype of PCa are poorly understood [10][11].

Tumor cells may develop various escape mechanisms that allow them to avoid recognition and destruction by the immune system. For example, the expression of checkpoint proteins (PD-1/PD-L1, CTLA-4, LAG3) by tumors can modulate the activity of immune infiltrate cells [11]. Tumors may also develop intrinsic cancer-cell signaling that can suppress infiltrating immune cells (WNT/β-catenin) and increase pro-tumorigenic immune cell infiltration (Tregs, M2 Macrophages) in the TME [12], [13]. Another mechanism exploited by tumors to avoid the recognition of cytotoxic T cells (CD8+) and antigen-presenting cells (APCs) is through loss of major histocompatibility complex class-I or class-II (MHC-I and MHC-II) [14].

Changes in MHC expression have been linked to tumor progression, poor prognosis, and reduced response to ICB in different malignancies [15], [16]. As classified by Garrido et al., the alteration in the MHC expression can be divided into two major mechanistic groups: tumors with “Soft” alterations are capable of recovering or upregulating MHC antigens after cytokine exposure (e.g., they have regulatory abnormalities); those with “Hard” alterations cannot recover MHC expression (e.g., they have structural defects) [17]. During tumor evolution, the infiltration of cytotoxic lymphocytes eliminates highly immunogenic tumor clones, causing a selection of surviving cell populations that have acquired MHC alterations through either “Soft” or “Hard” mechanistic alterations [18]. Low expression of MHC-I and -II has been associated with poor prognosis and resistance to anti-CTLA-4 and anti-PD-1, respectively [19], [20]. However, in PCa, there is presently limited information on the role of MHC-

I and MHC-II expression and ICB response and if the low expression of antigen presentation mechanism could better predict the lack of response to ICB in *CDK12*-altered patients.

In prostate cancer, *CDK12* inactivation is known to increase the immunogenicity of tumor cells, but the relationship between *CDK12* loss and MHC expression has not been investigated. Changes in MHC-I and -II expression are involved in tumor immune evasion in various types of cancer. There is also evidence that higher expression of MHC genes can identify tumors likely to respond to ICB [15], [16]. However, the molecular and genomic mechanisms responsible for reducing MHC expression are poorly understood. Hence, we hypothesize that variation in the expression of the MHC genes could explain the lack of response to ICB in *CDK12* defective tumors. The findings suggest that *CDK12* defective PCa expressing higher MHC levels have an active and inflamed tumor microenvironment with elevated immunomodulatory pathway expression and increased presence of effector T cells. We also found that tumors with decreased MHC expression also showed loss-of-heterozygosity (LOH) of MHC-I/-II and the *HLA* gene cluster on chromosome 6 associated with MHC expression and antigen presentation. Collectively, these data suggest that implementing a combined measure between *CDK12* mutation and the presence of MHC expression may better predict outcomes for prostate cancer tumors classified as eligible for ICB treatment based on *CDK12* subtype and normal antigen presentation function.

Methods

We used The CbioPortal for Cancer Genomics [21] to search primary (pPCa) and metastatic castration-resistant (mCRPC) prostate tumors with *CDK12* mutated sample cohorts and to download matched clinical information. The classification of samples having *CDK12* loss-of-function followed previous reports [7]–[9] based only on the presence of somatic mutations (non-synonymous mutations, deep deletions, and shallow deletions) in both

CDK12 alleles (*CDK12* defective) [6–8]. Only cohorts containing *CDK12* defective samples WES and with RNA-seq data were selected in the database of Genotypes and Phenotypes (dbGaP) database and applied for access under project ID 29255 (Additional file 1: Fig. S1, additional table 1).

Transcriptomic analysis

For the pPCa (TCGA-Prostate Adenocarcinoma, n = 48), we used the package recount2 to download summarized experiments objects containing the transcription-level RNA-Seq abundance matrix [22], [23]. For the mCRPC (SU2C, n = 10), we downloaded SRA Paired-End (PE) reads using the SRAToolkit [24]. The quality of the raw reads was then measured using the FASTQC program [25]. We quantified the transcripts using the software Salmon v1.6.0 [26]. The transcriptome index was built using the reference GRCh38 version of the human genome [27] and transcriptome [28], downloaded from ENSEMBL and GENCODE, following the manual instruction. We then used the Tximport v1.22.0 package to import the transcription-level abundance and estimate raw counts derived from the quantification step. The count data normalization, expression levels, and differential gene expression (DEG) analysis for pPCa and mCRPC cohorts were executed using the DESeq2 v1.34.0 [29], [30]. We used the clusterProfiler v4.2.1 to implement equally over-representation (ORA) enrichment analysis and gene set enrichment analysis (GSEA) of the DEGs and the whole transcriptome profile, respectively, using the Gene Ontology (GO) and Molecular Signatures Database (MSigDB) [31]–[36] (Fig. S1).

MHC expression

We performed a hierarchical clustering analysis using representative MHC genes. We observed two groups of *CDK12* defective tumors regarding MHC expression, as shown in

Additional file 1, Figure S1. We dichotomized expression levels below or above the first quartile for each gene; we then used this classification to generate the final logical values regarding the patient's MHC status ('High' or 'Low' expressed) (Additional file 1: Fig. S2)[37], [38]. For the quartile quantification, we used the normalized expression values of the classical genes that composed each MHC class (e.g., MHC-I: *HLA-A*, *HLA-B*, *HLA-C*; MHC-II: *HLA-DPA1*, *HLA-DPB1*, *HLA-DQA1*, *HLA-DQB1*, *HLA-DQB2*, *HLA-DRA*, *HLA-DRB5*, *HLA-DRB6*) [38]. Samples were classified as having MHC 'Low' expression when at least one gene composing each class was expressed at a low level. In mCRPC *CDK12*- defective, all tumors classified as MHC-High presented similar high expression of both MHC-I and -II; thus, we called these tumors just MHC High (henceforth, mCRPC *CDK12* defective MHC High). The summary values used to classify the tumors are shown in table S1. The final logical values are shown in additional tables 3, 4, 5, and 6.

Genomic profile

We downloaded SRA Paired-End (PE) reads for both pPCa (n=48) and mCRPC (n=10) and processed it as previously described. The GRChg38 reference was sorted using the SeqKit [39]. The final fastq files were then aligned to hg38 using bwa with a penalty for up to 3 mismatches per read [40], [41]. Sam files were converted to bam files and processed using samtools v1.16.1. To determine whether any MHC expression differences were related to genomic alterations, we used the FACETS (Fraction and Allele-Specific Copy Number Estimated from Tumor Sequencing) algorithm [42]. This approach uses matched normal-tumors WES and provides mutant allele-specific copy-number homozygous/heterozygous deletions, copy-number neutral loss-of-heterozygosity (LOH), allele-specific gain/amp in genomic loci associated with genes involved in antigen presentation (Additional table 11). Reference and variant allele read counts were extracted from the bam file for common, poly-

morphic SNPs downloaded from dbSNP (GRCh38p7) using FACETS *snp_pileup* function with a minimum threshold for mapping quality, the minimum threshold for the base quality, and minimum read depth of 15, 20, 20, respectively. The pre-processing followed the suggested recommendations from the manual, and genomic intervals of 150-250bp were used to avoid hyper-segmentation in high polymorphic neighborhood regions. Mutant allele-specific copy-number changes were declared when the points changes were greater than a predetermined critical value (cval) of 100 compared to constant copy-number regions [43], [44].

Digital cytometry

To investigate and quantify the immune cell composition in the TME of tumors having *CDK12* defects, we used the bulk tissue gene expression profiles (GEP) from RNA-seq data from both pPCa and mCRPC with the digital cytometry CIBERSORTx [45]–[47]. This program uses bulk tissue GEP, compares the data with prior knowledge of expression profiles from purified leukocytes, and estimates a tumor's relative immune abundance composition. We used the ‘signature matrix’ containing a validated leukocyte GEP of 22 human hematopoietic cell phenotypes, leukocyte gene signature matrix (LM22), to estimate the immune cell composition from the TME.

Computational and statistical analysis

We used a GNU/Linux environment to perform the quality control and quantify the raw reads to the human transcriptome. Subsequently, downstream analysis was performed in RStudio software (R Foundation for Statistical Computing, R v4.1.2). Pearson Correlation was used to analyze the normalized expression levels (coef. level = 0.95). A gene was considered differentially expressed when log2 foldchange > 1 expressed from the reference

group with a *p*-adjusted value < 0.05. For the enrichment analysis, we used a cutoff value of 0.05.

Results

Clinical analysis

The material under study was obtained retrospectively from the cBioPortal public domain. The 58 cases, defined according to NCCN criteria, had the intermediate-risk disease (clinical stage T2b, or T2c, Gleason score of 7, or PSA = 10–20 ng/ml) and high-risk disease (clinical stage T3a or higher, Gleason score 8–10, or PSA >20 ng/ml). We divided our cases into two cohorts, primary and metastatic tumors (Additional table 1). The pPCa cohort comprises 48 cases, approximately 63 years old (median), with clinical stages ranging from T2b to T4. Within these tumors, 62.5% were classified as MHC I high and 47.916% as MHC II high. The pPCa *CDK12*-defective MHC-I High exhibited a trend towards better overall survival compared to the MHC lower expression group ($p > 0.05$, Additional file 1: Figure S3).

The mCRPC cohort comprises 10 cases, approximately 63 years old (median), with Gleason scores ranging from 6 to 9. Among them, 60% were classified as MHC High. The metastatic sites were bone, liver, lymph nodes, and soft tissues, and 50% of the tumors were treated with taxanes and 40% with Abiraterone plus enzalutamide. Tumors with higher MHC expression exhibited apparently better overall survival when compared to the MHC lower expression group ($p > 0.5$, Additional file 1: Figure S3).

Transcriptomics

Our working hypothesis for this study is that variation in the expression of the MHC genes among *CDK12* defective tumors could provide predictive information on poor ICB

responses in this molecular subtype of prostate cancer. To investigate MHC expression levels in PCa further, we compared the transcriptomics of prostate tumors, including *CDK12* defective (*CDK12* defective) prostate tumors, classified as "MHC High" (top 75% quartile) to the transcriptomics of tumors classified as having a low expression of MHC genes (bottom 25% quartile).

CDK12 defective MHC-I/-II High-expression tumors showed distinct transcriptome profiles with upregulation of IFN-γ-responsive genes and an inflamed TME

We first compared the transcriptome of *CDK12* defective tumors classified as MHC-High and MHC-Low (Fig 1a-c, Additional file 1: Fig. S2). The 48 primary PCa *CDK12* defective MHC-I High showed 1319 upregulated and 2153 downregulated genes (Additional table 7, 8) and showed four apparent clusters (Fig. 1a). The upper cluster (I) has *IGHV* and *IGLV* over-expressed genes linked to *CDK12* MHC I high. The central clusters (II, III) have four *HLA* genes overexpressed in the MHC I high group, which supports our classification based on *CDK12* defective MHC expression (e.g., *HLA-A*, *HLA-B*, *HLA-C*). Also, this cluster showed upregulation of many genes related to antigen presentation and CD8+ T cell activity (Fig. 1a). The lower cluster (IV) has 14 downregulated genes when MHC I is highly expressed. Likewise, *CDK12* defective MHC-II High exhibited 1129 upregulated and 580 downregulated genes (Additional tables 7, 9). Our comparison showed two clusters (Fig. 1b). The upper cluster showed the upregulation of genes related to cytotoxicity, immune cell migration, and immune suppression (Fig. 1b).

Analysis of ten mCRPC tumors identified 230 upregulated and 46 downregulated genes that were differentially expressed in *CDK12* defective MHC-high (Additional tables 7, 10) and showed two distinct clusters (Fig. 1c). The lower cluster showed the upregulation of genes linked to innate and adaptative immune response CD4+ and CD8+ T cell activity (Fig.

1c). In conclusion, for both primary PCa and metastatic CRPC, *CDK12* defective PCa that express higher MHC levels was associated with transcriptomic changes that indicate a general pattern of activation of IFN-γ-responsive and cytotoxic activity genes.

To better understand the transcriptional alterations in *CDK12* defective tumors classified as MHC-I/-II high-expressed, we used ORA and GSEA analysis to identify potential functional associations of expression changes associated with differentially expressed genes. In primary PCa, tumors with *CDK12* defective MHC-I and MHC-II high-expressed showed significative enrichment of pathways related to activation of immune cells and antigen presentation by MHC-I and MHC-II, as expected (Fig. 1d, e, Additional table 8, 9). Furthermore, GSEA results showed activation of many Hallmarks pathways in *CDK12* defective MHC-I high-expressed (e.g., Epithelial-Mesenchymal Transition, Inflammatory Response, Interferon Gamma Response, Interferon Alpha Response, TNFA Signaling via NFKB, P53, and IL2/STAT5 Signaling (Fig. 2a, Additional table 8). In addition, the *CDK12* defective MHC-II High group had similar pathway activation but with the addition of Allograft Rejection (Fig. 2b, Additional table 9).

The *CDK12* defective metastatic group with MHC high-expressed showed enrichment of cytotoxicity and adaptative cytotoxicity immune response (Fig. 1f, Additional table 10). In addition, GSEA results showed activation of various Hallmarks and Reactome pathways (e.g., Allograft Rejection, Interferon Gamma Response, Inflammatory Response, Interferon Alpha Response, IL2/STAT5 Signaling, Apoptosis, TCR Signaling, Interleukin 10 Signaling, Constitutive Signaling by Aberrant PI3K in Cancer, and the suppressive PD1 Signaling pathway) (Fig. 2c-d, Additional table 10). Our transcriptomic analysis suggests that *CDK12* defective PCa expressing high MHC genes display the activation of various pathways associated with an active and inflamed tumor microenvironment.

CDK12 defective MHC-I/-II High groups exhibited tumor microenvironment with high expression of chemokines and immunomodulatory genes.

We investigate the difference between chemokines and immunomodulatory gene expression to elucidate the underlying immunologic signature in TME of CDK12 defective tumors expressing high MHC genes. In primary PCa, the *CDK12* defective MHC-I High exhibited upregulation of many chemokines linked to APCs and effector T cell migration (Addition file 1, Figure S4**)** and the immunomodulatory genes *HAVCR2* (*TIM3*) and *IDO1*. (Fig. 3a-b). Also, the MHC-II high group presented increased expression of chemokines related to Natural killer, T effector cell, and B cell infiltration (Addition file 1, Fig. S2, Figure S5), and the immunomodulatory genes *CD274* (*PD-L1*), *HAVCR2* (*TIM3*), and *IDO1* (Fig. 2c-e). Based on Pearson Correlation analysis, we observed a significant positive correlation between MHC-I complex genes and *IDO1* but with no other investigated gene (Addition file 1, Figure S7a). Interestingly, among the MHC-II genes, correlation analysis showed a significant positive association between the expression of the MHC-II complex and the immunomodulatory genes *CD274* (*PD-L1*), *IDO1*, and *HAVCR2* (*TIM3*) (Figure S7b).

The *CDK12* defective metastatic group with high expression of MHC showed high expression of chemokines (Addition file 1, Figure S6) and the immunomodulatory gene *CD274* (*PD-L1*) (Fig. 3f). Furthermore, we observed a significant positive association between the immunomodulatory genes *HAVCR2* (*TIM3*) and *CTLA4*, *LAG3*, and MHC-I and -II genes (Addition file 1, Figure S7c-d). As shown, *CDK12* defective tumors' expression of higher levels of MHC genes shows a pattern of upregulation of chemokine and immunomodulatory mechanisms.

CDK12 defective MHC-I/-II High CDK12 defective tumors showed distinct immune cell infiltrate in the TME.

Our transcriptomics analysis predicted that *CDK12* defective tumors expressing high levels of MHC-I/-II genes would display enrichment of immune cells with high effector and cytotoxic activity and the co-inhibitory expression of inhibitory pathways by tumor cells (Figures 1, 2, 3). We used *in silico* cytometry (CIBERSORTx) to test this hypothesis and to estimate the immune cell composition in the TME of *CDK12* defective tumors expressing high levels of MHC-I/-II genes.

We investigated whether tumors expressing high MHC-I and -II levels affected the variation in immune cell composition in *CDK12* defective tumors in both cohorts. In primary PCa, *CDK12* defective MHC-I high-expressed showed a significant increase in the composition of Naïve B cells, CD8+ T cells, and γδ T cells. In contrast, the reduced composition of Mastocytes (Fig. 4a). In comparison, the MHC-II high-expressed group exhibited an increase of γδ T cells and reduced composition of Plasma cells and M0 macrophages (Figure 4b).

Additionally, the *CDK12* defective metastatic group with high expression of MHC showed a significative increased composition of CD8+ T cell and M1 Macrophages (Figure 4c). Our results generally indicate that *CDK12* defective PCa expressing higher levels of MHC displayed increased APCs and effector lymphocytes traffic in their TME.

Genomics alterations of MHC-I/-II region associated with defective CDK12

During tumor evolution, the infiltration of cytotoxic lymphocytes eliminates highly immunogenic tumor clones, causing a preferential selection and survival of cell populations that have acquired MHC alterations. To determine whether the low levels of MHC-I/-II genes in *CDK12* defective tumors were derived from somatic genomic alterations affecting antigen

presentation genes, we used an allele-specific copy number algorithm to estimate the copy number profile of *CDK12* defective tumors expressing low levels of MHC-I/-II genes. The algorithm incorporates quantitative analysis of RNA-seq data derived from MHC-I/-II and *HLA* genes on chromosome 6 together with several other genes, such as *PTEN*, that are commonly subject to LOH in PCa [48]. Estimates include the determination of the relative clonality of allele-specific copy number alterations based on the fraction of tumor cells bearing LOH.

WES of primary PCa revealed both subclonal allele-specific copy-neutral losses of heterozygosity (CN-LOH) and complete loss of heterozygosity (LOH) events affecting MHC-I/-II and *HLA* genes on chromosome 6. Both major clonal and minor subclonal events were detected by comparing the copy number to the estimated cellular fraction of tumor cells harboring the copy number alteration (Table 1 and Figure S9). One example is illustrated by tumor TCGA-KK-A8IA in which only one major clonal event was detected with a cellular fraction = 0.833, and LOH events were detected on chromosomes 2, 5, and 10. While TCGA-YL-A8HO revealed four subclonal events, capturing biallelic loss, CN-LOH, and LOH in chromosomes 2, 5, 6, 15, and 16. Tumors expressing lower levels of MHC-I/II genes may be associated with the somatic genomic LOH events affecting regional transcriptional regulators of MHC expression and the cis-acting regulatory components of the MHC (Table 1). Two patients also showed subclonal complete loss of the *B2M* locus (ID: TCGA-EJ-8471, cellular fraction = 0.37; TCGA-YL-A8HO, cellular fraction = 0.27. Table 1). Interestingly, *B2M* is an important component of the MHC-I complex, and mutations of this gene have previously been associated with ICB resistance [49].

In contrast to primary PCa, metastatic tumors harboring *CDK12* mutation expressing low levels of MHC-I/II showed allele-specific copy number gains in the MHC-I/I*I* complex and key regulators of MHC expression (Table 2 and Figure S10). Interestingly, one patient

showed a clonal LOH event at the *JAK2* and *B2M* loci (ID: 5115615, cellular fraction = 0.90).

These data indicate that low expression of MHC in primary tumor clones appears to be associated with frequent somatic CN-LOH and LOH subclonal genomic alterations in primary tumors harboring *CDK12* mutation. While metastatic tumors revealed both LOH and high copy-number gains affecting antigen presentation genes and their regulators. Therefore, these subclonal CN-LOH and LOH events are associated with impaired MHC expression that may contribute to reducing tumor immunogenicity.

Discussion

In prostate cancer, *CDK12* inactivation is known to increase the immunogenicity of tumor cells [9], [50]–[53]. Changes in MHC-I and -II expression are involved in tumor immune evasion in various types of cancer [38], [54]–[56]. Using RNA-seq data, we observed two groups of *CDK12* defective tumors regarding MHC expression. Tumors expressing higher levels of MHC showed the activation of multiple pathways associated with the immune system, significantly high expression of immunomodulatory genes, and increased CD8+ T cells, B cells, γδ T cells, and M1 Macrophages composition in their TME. Also, Tumors with low MHC expression showed allele-specific copy-number alteration in genes involved in regulating MHC expression and antigen presentation.

Analysis of the clinical data showed that higher expression of MHC genes in pPCa and mCRPC, respectively, exhibited a trend towards better overall survival when compared to the MHC lower expression group ($p > 0.05$, Fig. S3). Several studies have found similar expression relationships of the *MHC-I* and *-II* genes associated with better clinical outcomes and different resistance mechanisms [20], [57], [58]. Lack of MHC-I expression in melanoma was linked to higher odds of progressive disease and resistance to anti-CTLA4 but not anti-

PD1 [20]. In the same study, expression of MHC-II in tumors was associated with tumors more likely to respond to anti-PD1 treatment. MHC-II expression was linked to a positive outcome in Hodgkin Lymphoma treated with nivolumab (anti-PD1) [57]. Park et al. showed that MHC-II positivity in tumor cells was associated with better disease-free survival in patients with lymph node metastasis [58]. From a practical standpoint, these results suggest that analysis of MHC-I and -II expression levels could be developed to determine whether *CDK12* defective prostate tumors expressing higher levels of MHC genes are more likely to respond to ICB treatments.

Transcriptomic signatures associated with MHC expression variation have been described in different tumor types [38]. These signatures capture the activity of genes and biological pathways related to tumor cells' cross-talk with the TME and appear to correlate with clinical responses to ICB [20], [38], [59]–[61]. Ayers *et al.* proposed a gene expression profile with eighteen genes relevant to predicting the clinical outcome of anti-PD1 therapy [59]. This IFN-γ gene signature in pretreatment tumor biopsies was associated with better results in melanoma, head-and-neck squamous cell carcinoma, and gastric cancer treated with pembrolizumab. In our study, the *CDK12* patient tumors expressing high levels of MHC genes showed the presence IFN-γ gene signature, which might reflect a better response to anti-PD1 therapy (Figure S8). Our results also showed the activation of pathways related to IFN-γ response in both the pPCA and mCRPC cohorts (Fig. 1B, D, F, Fig. 3B, D, Fig. 4B-C).

An IFN-γ gene signature can alternatively activate the expression immunomodulatory mechanisms and promote adaptative resistance to therapeutic anti-PD1 [62], [63]. IFN-γ is a central actor in the elimination phase during immunoediting [64]. However, exacerbated levels of IFN-γ are also associated with developing protumor molecular mechanisms leading to an immunosuppressive and tolerogenic TME [63]. We identified the upregulation of immunomodulatory molecules, such as *IDO1*, *TIM3,* and *CD274(PD-L1),* in both prostate

tumors expressing higher levels of MHC-I and -II genes (Fig. 2). Interestingly, the *CDK12* patient tumors expressing high levels of MHC genes showed the presence IFN-γ gene signature, including upregulation of a non-classical MHC molecule (*HLA-E*), which is known regulator of NK cell and CTL [65], [66]. We also found a link between *IGHV* and *IGLV* overexpressed genes in a group of the *CDK12* defective pPCa expressing high levels of MHC-I (Fig. 1A, upper cluster I). The production of Ig by tumor cells (cancer-derived Ig) is described in various tumors and prostate cancer [67]–[70]. Also, cancer-derived Ig may act as checkpoint proteins and inhibit effector T cells and NK cells [68], [71]. Our findings indicate the presence of an acquired resistance mechanism in a subset of *CDK12* defective prostate tumors expressing high levels of MHC genes. We suppose that measuring the basal expression of MHC genes could be developed as a biomarker to characterize *CDK12* patient samples with a previously inflamed environment and which would reflect the expression of immunomodulatory genes linked to resistance to anti-PD1.

The expression of MHC molecules plays a pivotal role in providing the signals necessary to recognize and activate the immune system against tumor neoantigens and is essential to controlling tumor growth through cytotoxic activity [64], [72]. We found a higher abundance of CD8+ T cells in *CDK12* defective tumors expressing high levels of MHC genes (Figure 4). This result may either indicate the dependence of CD8+ T cells in MHC-I antigen presentation or suggest that enhanced CD4+ Th infiltrate could support the continued accumulation of CD8+ CTLs in the tumor microenvironment [60]. Interestingly, *CDK12* pPCa with high expression of both MHC-I and -II genes showed increased levels of γδ T cells (Figure 4a-b). The basal effector immune cell population, such as γδ T cells in pPCa, may contribute to IFN-γ signaling and indicate the dependence of the MHC-unrestricted recognition role of γδ T cells and its presence in the TME [20], [73].

The loss of MHC expression could be derived from two different disruption means [74]. First, regulatory abnormalities downregulate the expression of MHC genes through mechanisms that do not affect the genomic structure of HLA genes. In such cases, specific T-cells can recover the MHC expression-mediated response (e.g., IFN-γ signaling). Second, during tumor evolution, the infiltration of cytotoxic lymphocytes eliminates tumor clones high immunogenic, causing a selection of clones that may present structural alteration, or "Hard" lesions, in the MHC loci or other genomic regions (e.g., *B2M*, *IFN*, *STAT*) distinct from the derived clone [49].

Genomic studies of chromosome 6 in various cancers suggest reduced MHC expression is often associated with genetic and LOH aberrations that may result in reduced antigen presentation and, thus, facilitate immune evasion [15], [75]. In keeping with these data, our WES of pPCa and mCRPC revealed CN-LOH and LOH in *CDK12* defective tumors expressing low levels of MHC-I/II genes at known regulators of MHC expression and the components of the MHC (Table 1-2). Two pPCa patients also showed complete loss of the *B2M* locus, while one mCRPC exhibited a LOH event at the *B2M*, an important component of the MHC-I complex [49]. These results indicate that after selection, the low expression of MHC genes is derived from tumor clones harboring "Hard" genomics alterations comprising loci involved in normal MHC expression. Therefore, these clones will be invisible to the immune system and contribute to tumor progression [18].

This study has a number of limitations. First, future studies in a large number of patients harboring CDK12 mutations are needed to address potential statistical bias regarding our low number of patients. Second, we did not address the potential molecular mechanism underlying the alteration of the low expression of MHC in *CDK12* defective prostate cancer, including epigenetic alterations and miRNA activity. Further studies are needed to approach the causes of MHC disruption derived from "Soft" alterations that occurs in *CDK12* defective

prostate cancer. Third, because the non-tumor cell content was not defined in this study, we could not establish a limit for the contribution of the *CDK12* defective tumor cells and TME to the MHC expression since the RNA-seq relies on data from bulk tissue [76].

Conclusion

We distinguished two sets of *CDK12* defective tumors based on differential MHC expression levels. Our data suggest that *CDK12* defective PCa expressing higher levels of classical MHC genes have an active and inflamed tumor microenvironment with elevated immunomodulatory pathway expression and increased presence of effector T cells. Tumors with decreased MHC expression showed copy-number alteration in genes that regulate MHC expression and antigen presentation. More extensive *in vitro* and *in vivo* investigations are required to relate this molecular subtype to potential actionable immunomodulatory mechanisms or possible therapeutic targets in PCa. These findings also support investigations into the clinical use of MHC expression levels in *CDK12* defective prostate cancer to identify tumors likely to respond to ICB treatment.

List of abbreviations

ADT: Androgen Deprivation therapy

APC: Antigen-presenting cells

CDK12: Cyclin-dependent Kinase 12

CN-LOH: Copy-neutral loss of heterozygosity

dbGaP: The database of Genotypes and Phenotypes

DDR: **DNA damage repair**

DEGs: Differentially expressed genes

FACETS: Fraction and Allele-Specific Copy Number Estimated from Tumor Sequencing

FDR: False discovery rate

GEP: Gene expression profile

GO: Gene ontology

ICB: Immune-checkpoint blockade

LM22: Leukocyte gene signature matrix

LOH: loss of heterozygosity

mCRPC: Metastatic Castration-Resistant Prostate Cancer

MHC: Major histocompatibility complex

MSigDB: Molecular Signature Database

NCCN: National Comprehensive Cancer Network

ORA: Over-representation analyses

PCa: Prostate Cancer

PE: Paired-end

pPCa: Primary prostate cancer

PRAD: Prostate Adenocarcinoma

PSA: Prostate-specific antigen

TCGA-PRAD: The Cancer Genome Atlas

TME: Tumor microenvironment

LOH*:* Loss-of-Heterozygosity

Ethics approval and consent to participate

Not applicable.

Consent for publication

Not applicable.

Availability of data and materials

The original dataset is deposited in the database of Genomic and Phenotypes (dbGaP) under accession numbers phs000178.v11.p8.c1, phs000915.v2.p2.c1. The original clinical information of both cohorts is deposited in the CbioPortal [77] and GDC Portal [78]. All other data supporting the conclusions of this article are included within the article and its additional files.

Competing interests

The authors declare that they have no competing interests.

Funding

This work is partly funded by *Fundação de Amparo à Pesquisa de São Paulo (FAPESP)* (2019/22912-8). W.L.D. is funded by the *FAPESP* (2021/12271-5). L.P.C. is funded by *FAPESP* (2020/12816-9). S. L. B. and J.A.S. are Research Career Awardees of *Conselho Nacional de Desenvolvimento Científico e Tecnológico (CNPq).*

Authors' contributions

Conception: W. L. D. and J. A. S

Interpretation or analysis of data: W. L. D., S. L. B., and J. A. S

Preparation of the manuscript: W. L. D. and J. A. S.

Revision for important intellectual content: L. P. C, C. M. M., and R. B. R.

Supervision: S. L. B. and J. A. S.

Acknowledgments

The authors are grateful to L. A. F. B. and S. P. F. B. for the informatic technical support in the early stage of the project; Genomic and Molecular laboratory/PUCRS for technical assistance, and dbGap and the Cbioportal for archiving and distributing the data from the above-cited studies.

References

[1] R. J. Rebello *et al.*, "Prostate cancer," *Nat Rev Dis Primers*, vol. 7, no. 1, Dec. 2021, doi: 10.1038/s41572-020-00243-0.

[2] M. C. S. Wong *et al.*, "Global Incidence and Mortality for Prostate Cancer: Analysis of Temporal Patterns and Trends in 36 Countries," *Eur Urol*, vol. 70, no. 5, pp. 862–874, Nov. 2016, doi: 10.1016/j.eururo.2016.05.043.

[3] M. Binnewies *et al.*, "Understanding the tumor immune microenvironment (TIME) for effective therapy," *Nat Med*, vol. 24, no. 5, pp. 541–550, May 2018, doi: 10.1038/s41591-018-0014-x.

[4] C. M. Melo, T. Vidotto, L. P. Chaves, W. Lautert-Dutra, R. B. dos Reis, and J. A. Squire, "The role of somatic mutations on the immune response of the tumor microenvironment in prostate cancer," *Int J Mol Sci*, vol. 22, no. 17, 2021, doi: 10.3390/ijms22179550.

[5] T. N. Schumacher and R. D. Schreiber, "Neoantigens in cancer immunotherapy," *Science*, vol. 348, no. 6230. American Association for the Advancement of Science, pp. 69–74, Apr. 03, 2015. doi: 10.1126/science.aaa4971.

[6] Y. M. Wu *et al.*, "Inactivation of CDK12 Delineates a Distinct Immunogenic Class of Advanced Prostate Cancer," *Cell*, vol. 173, no. 7, pp. 1770-1782.e14, Jun. 2018, doi: 10.1016/j.cell.2018.04.034.

[7] B. Nguyen *et al.*, "Pan-cancer Analysis of CDK12 Alterations Identifies a Subset of Prostate Cancers with Distinct Genomic and Clinical Characteristics," *Eur Urol*, vol. 78, no. 5, pp. 671–679, Nov. 2020, doi: 10.1016/j.eururo.2020.03.024.

[8] P. Rescigno *et al.*, "Characterizing CDK12-mutated prostate cancers A C," *Clinical Cancer Research*, vol. 27, no. 2, pp. 566–574, Jan. 2021, doi: 10.1158/1078-0432.CCR-20-2371.

[9] E. S. Sokol *et al.*, " Pan-Cancer Analysis of CDK12 Loss-of-Function Alterations and Their Association with the Focal Tandem-Duplicator Phenotype ," *Oncologist*, vol. 24, no. 12, pp. 1526–1533, Dec. 2019, doi: 10.1634/theoncologist.2019-0214.

[10] E. S. Antonarakis *et al.*, "CDK12-Altered Prostate Cancer: Clinical Features and Therapeutic Outcomes to Standard Systemic Therapies, Poly (ADP-Ribose) Polymerase Inhibitors, and PD-1 Inhibitors," 2020. [Online]. Available: https://doi.org/10.

[11] S. Spranger and T. F. Gajewski, "Mechanisms of Tumor Cell-Intrinsic Immune Evasion," *Annu. Rev. Cancer Biol*, vol. 2, pp. 213–228, 2018, doi: 10.1146/annurev-cancerbio.

561 [12] X. Li, Y. Xiang, F. Li, C. Yin, B. Li, and X. Ke, "WNT/β-catenin signaling pathway regulat-
562 ing T cell-inflammation in the tumor microenvironment," *Frontiers in Immunology*,
563 vol. 10, no. SEP. Frontiers Media S.A., Sep. 01, 2019. doi: 10.3389/fimmu.2019.02293.
564 [13] B. L. Horton, T. B. Fessenden, and S. Spranger, "Tissue Site and the Cancer Immunity
565 Cycle," *Trends in Cancer*, vol. 5, no. 10. Cell Press, pp. 593–603, Oct. 01, 2019. doi:
566 10.1016/j.trecan.2019.07.006.
567 [14] N. McGranahan *et al.*, "Allele-Specific HLA Loss and Immune Escape in Lung Cancer
568 Evolution," *Cell*, vol. 171, no. 6, pp. 1259-1271.e11, Nov. 2017, doi:
569 10.1016/j.cell.2017.10.001.
570 [15] K. Dhatchinamoorthy, J. D. Colbert, and K. L. Rock, "Cancer Immune Evasion Through
571 Loss of MHC Class I Antigen Presentation," *Front Immunol*, vol. 12, Mar. 2021, doi:
572 10.3389/fimmu.2021.636568.
573 [16] J. Thibodeau, M.-C. Bourgeois-Daigneault, and R. Lapointe, "Targeting the MHC Class
574 II antigen presentation pathway in cancer immunotherapy," *Oncoimmunology*, vol. 1,
575 no. 6, pp. 908–916, Sep. 2012, doi: 10.4161/onci.21205.
576 [17] F. Garrido and N. Aptsiauri, "Cancer immune escape: MHC expression in primary tu-
577 mours versus metastases," *Immunology*, vol. 158, no. 4. Blackwell Publishing Ltd, pp.
578 255–266, Dec. 01, 2019. doi: 10.1111/imm.13114.
579 [18] I. Algarra, F. Garrido, and A. M. Garcia-Lora, "MHC heterogeneity and response of
580 metastases to immunotherapy," *Cancer and Metastasis Reviews*, vol. 40, no. 2.
581 Springer, pp. 501–517, Jun. 01, 2021. doi: 10.1007/s10555-021-09964-4.
582 [19] N. F. S. Watson *et al.*, "Immunosurveillance is active in colorectal cancer as
583 downregulation but not complete loss of MHC class I expression correlates with a
584 poor prognosis," *Int J Cancer*, vol. 118, no. 1, pp. 6–10, Jan. 2006, doi:
585 10.1002/ijc.21303.
586 [20] S. J. Rodig *et al.*, "MHC proteins confer differential sensitivity to CTLA-4 and PD-1
587 blockade in untreated metastatic melanoma," 2018. [Online]. Available:
588 https://www.science.org
589 [21] J. Gao *et al.*, "Integrative analysis of complex cancer genomics and clinical profiles
590 using the cBioPortal," *Sci Signal*, vol. 6, no. 269, Apr. 2013, doi:
591 10.1126/scisignal.2004088.
592 [22] E. L. Imada *et al.*, "Recounting the FANTOM Cage Associated Transcriptome," *bioRxiv*,
593 2019, doi: 10.1101/659490.
594 [23] A. Abeshouse *et al.*, "The Molecular Taxonomy of Primary Prostate Cancer," *Cell*, vol.
595 163, no. 4, pp. 1011–1025, Nov. 2015, doi: 10.1016/j.cell.2015.10.025.
596 [24] "ncbi/sra-tools: SRA Tools." https://github.com/ncbi/sra-tools (accessed May 11,
597 2022).
598 [25] "Babraham Bioinformatics - FastQC A Quality Control tool for High Throughput Se-
599 quence Data." https://www.bioinformatics.babraham.ac.uk/projects/fastqc/ (ac-
600 cessed May 11, 2022).
601 [26] R. Patro, G. Duggal, M. I. Love, R. A. Irizarry, and C. Kingsford, "Salmon provides fast
602 and bias-aware quantification of transcript expression," *Nat Methods*, vol. 14, no. 4,
603 pp. 417–419, 2017, doi: 10.1038/nmeth.4197.
604 [27] "Ensembl Genome Browser." http://ftp.ensembl.org/pub/release-
605 105/fasta/homo_sapiens/dna/Homo_sapiens.GRCh38.dna.primary_assembly.fa.gz
606 (accessed May 11, 2022).

[28] "European Bioinformatics Institute," *Gencode_human*. https://ftp.ebi.ac.uk/pub/databases/gencode/Gencode_human/release_39/gencode.v39.transcripts.fa.gz (accessed May 11, 2022).

[29] M. I. Love, W. Huber, and S. Anders, "Moderated estimation of fold change and dispersion for RNA-seq data with DESeq2," *Genome Biol*, vol. 15, no. 12, Dec. 2014, doi: 10.1186/s13059-014-0550-8.

[30] A. Zhu, J. G. Ibrahim, and M. I. Love, "Heavy-Tailed prior distributions for sequence count data: Removing the noise and preserving large differences," *Bioinformatics*, vol. 35, no. 12, pp. 2084–2092, Jun. 2019, doi: 10.1093/bioinformatics/bty895.

[31] T. Wu *et al.*, "clusterProfiler 4.0: A universal enrichment tool for interpreting omics data," *The Innovation*, vol. 2, no. 3, Aug. 2021, doi: 10.1016/j.xinn.2021.100141.

[32] A. Liberzon, C. Birger, H. Thorvaldsdóttir, M. Ghandi, J. P. Mesirov, and P. Tamayo, "The Molecular Signatures Database Hallmark Gene Set Collection," *Cell Syst*, vol. 1, no. 6, pp. 417–425, Dec. 2015, doi: 10.1016/j.cels.2015.12.004.

[33] A. Subramanian *et al.*, "Gene set enrichment analysis: A knowledge-based approach for interpreting genome-wide expression profiles," 2005. [Online]. Available: www.pnas.orgcgidoi10.1073pnas.0506580102

[34] P. Khatri, M. Sirota, and A. J. Butte, "Ten years of pathway analysis: Current approaches and outstanding challenges," *PLoS Computational Biology*, vol. 8, no. 2. Feb. 2012. doi: 10.1371/journal.pcbi.1002375.

[35] S. Carbon *et al.*, "The Gene Ontology Resource: 20 years and still GOing strong," *Nucleic Acids Res*, vol. 47, no. D1, pp. D330–D338, Jan. 2019, doi: 10.1093/nar/gky1055.

[36] C. Soneson, M. I. Love, and M. D. Robinson, "Differential analyses for RNA-seq: transcript-level estimates improve gene-level inferences," *F1000Res*, vol. 4, p. 1521, Dec. 2015, doi: 10.12688/f1000research.7563.1.

[37] L. A. Koopman, W. E. Corver, A. R. van der Slik, M. J. Giphart, and G. J. Fleuren, "Multiple Genetic Alterations Cause Frequent and Heterogeneous Human Histocompatibility Leukocyte Antigen Class I Loss in Cervical Cancer," *Journal of Experimental Medicine*, vol. 191, no. 6, pp. 961–976, Mar. 2000, doi: 10.1084/jem.191.6.961.

[38] E. Schaafsma, C. M. Fugle, X. Wang, and C. Cheng, "Pan-cancer association of HLA gene expression with cancer prognosis and immunotherapy efficacy," *Br J Cancer*, vol. 125, no. 3, pp. 422–432, Aug. 2021, doi: 10.1038/s41416-021-01400-2.

[39] W. Shen, S. Le, Y. Li, and F. Hu, "SeqKit: A Cross-Platform and Ultrafast Toolkit for FASTA/Q File Manipulation," *PLoS One*, vol. 11, no. 10, p. e0163962, Oct. 2016, doi: 10.1371/journal.pone.0163962.

[40] M. H. Bailey *et al.*, "Comprehensive Characterization of Cancer Driver Genes and Mutations," *Cell*, vol. 173, no. 2, pp. 371-385.e18, Apr. 2018, doi: 10.1016/j.cell.2018.02.060.

[41] M. Montesion *et al.*, "Somatic HLA Class I Loss Is a Widespread Mechanism of Immune Evasion Which Refines the Use of Tumor Mutational Burden as a Biomarker of Checkpoint Inhibitor Response," *Cancer Discov*, vol. 11, no. 2, pp. 282–292, Feb. 2021, doi: 10.1158/2159-8290.CD-20-0672.

[42] R. Shen and V. E. Seshan, "FACETS: allele-specific copy number and clonal heterogeneity analysis tool for high-throughput DNA sequencing," *Nucleic Acids Res*, vol. 44, no. 16, pp. e131–e131, Sep. 2016, doi: 10.1093/nar/gkw520.

652 [43] C. Villarroya-Beltri *et al.*, "Biallelic germline mutations in MAD1L1 induce a syndrome
653 of aneuploidy with high tumor susceptibility," *Sci Adv*, vol. 8, no. 44, Nov. 2022, doi:
654 10.1126/sciadv.abq5914.
655 [44] Y. R. Murciano-Goroff *et al.*, "Reversion mutations in germline BRCA1/2-mutant tu-
656 mors reveal a BRCA-mediated phenotype in non-canonical histologies," *Nat Commun*,
657 vol. 13, no. 1, p. 7182, Nov. 2022, doi: 10.1038/s41467-022-34109-8.
658 [45] B. Chen, M. S. Khodadoust, C. L. Liu, A. M. Newman, and A. A. Alizadeh, "Profiling tu-
659 mor infiltrating immune cells with CIBERSORT," in *Methods in Molecular Biology*, vol.
660 1711, Humana Press Inc., 2018, pp. 243–259. doi: 10.1007/978-1-4939-7493-1_12.
661 [46] A. M. Newman *et al.*, "Robust enumeration of cell subsets from tissue expression pro-
662 files," *Nat Methods*, vol. 12, no. 5, pp. 453–457, Apr. 2015, doi: 10.1038/nmeth.3337.
663 [47] CIBERSORTx, "CIBERSORTx," *CIBERSORTx*. https://cibersortx.stanford.edu/ (accessed
664 May 11, 2022).
665 [48] T. Jamaspishvili *et al.*, "Clinical implications of PTEN loss in prostate cancer," *Nat Rev*
666 *Urol*, vol. 15, no. 4, pp. 222–234, Apr. 2018, doi: 10.1038/nrurol.2018.9.
667 [49] J. M. Zaretsky *et al.*, "Mutations Associated with Acquired Resistance to PD-1 Block-
668 ade in Melanoma," *New England Journal of Medicine*, vol. 375, no. 9, pp. 819–829,
669 Sep. 2016, doi: 10.1056/nejmoa1604958.
670 [50] T. L. Lotan and E. S. Antonarakis, "CDK12 deficiency and the immune microenviron-
671 ment in prostate cancer," *Clinical Cancer Research*, vol. 27, no. 2, pp. 380–382, Jan.
672 2021, doi: 10.1158/1078-0432.CCR-20-3877.
673 [51] Y. Li *et al.*, "CDK12/13 inhibition induces immunogenic cell death and enhances anti-
674 PD-1 anticancer activity in breast cancer," *Cancer Lett*, vol. 495, pp. 12–21, Dec. 2020,
675 doi: 10.1016/j.canlet.2020.09.011.
676 [52] S. J. Dubbury, P. L. Boutz, and P. A. Sharp, "CDK12 regulates DNA repair genes by sup-
677 pressing intronic polyadenylation," *Nature*, vol. 564, no. 7734, pp. 141–145, Dec.
678 2018, doi: 10.1038/s41586-018-0758-y.
679 [53] H. C. Juan, Y. Lin, H. R. Chen, and M. J. Fann, "Cdk12 is essential for embryonic devel-
680 opment and the maintenance of genomic stability," *Cell Death Differ*, vol. 23, no. 6,
681 pp. 1038–1048, Jun. 2016, doi: 10.1038/cdd.2015.157.
682 [54] F. Garrido, F. Ruiz-Cabello, and N. Aptsiauri, "Rejection versus escape: the tumor MHC
683 dilemma," *Cancer Immunology, Immunotherapy*, vol. 66, no. 2. Springer Science and
684 Business Media Deutschland GmbH, pp. 259–271, Feb. 01, 2017. doi:
685 10.1007/s00262-016-1947-x.
686 [55] N. Aptsiauri, F. Ruiz-Cabello, and F. Garrido, "The transition from HLA-I positive to
687 HLA-I negative primary tumors: the road to escape from T-cell responses," *Current*
688 *Opinion in Immunology*, vol. 51. Elsevier Ltd, pp. 123–132, Apr. 01, 2018. doi:
689 10.1016/j.coi.2018.03.006.
690 [56] M. Montesion *et al.*, "Somatic hla class i loss is a widespread mechanism of immune
691 evasion which refines the use of tumor mutational burden as a biomarker of check-
692 point inhibitor response," *Cancer Discov*, vol. 11, no. 2, pp. 282–292, Feb. 2021, doi:
693 10.1158/2159-8290.CD-20-0672.
694 [57] M. G. M. Roemer *et al.*, "JOURNAL OF CLINICAL ONCOLOGY Major Histocompatibility
695 Complex Class II and Programmed Death Ligand 1 Expression Predict Outcome After
696 Programmed Death 1 Blockade in Classic Hodgkin Lymphoma," 2018, doi:
697 10.1200/JCO.

698 [58] I. A. Park *et al.*, "Expression of the MHC class II in triple-negative breast cancer is as-
699 sociated with tumor-infiltrating lymphocytes and interferon signaling," *PLoS One*, vol.
700 12, no. 8, p. e0182786, Aug. 2017, doi: 10.1371/journal.pone.0182786.
701 [59] M. Ayers *et al.*, "IFN-γ-related mRNA profile predicts clinical response to PD-1 block-
702 ade," *Journal of Clinical Investigation*, vol. 127, no. 8, pp. 2930–2940, Aug. 2017, doi:
703 10.1172/JCI91190.
704 [60] D. B. Johnson *et al.*, "Melanoma-specific MHC-II expression represents a tumour-
705 autonomous phenotype and predicts response to anti-PD-1/PD-L1 therapy," *Nat*
706 *Commun*, vol. 7, Jan. 2016, doi: 10.1038/ncomms10582.
707 [61] D. B. Johnson *et al.*, "Quantitative spatial profiling of PD-1/PD-L1 interaction and HLA-
708 DR/IDO-1 predicts improved outcomes of anti-PD-1 therapies in metastatic melano-
709 ma," *Clinical Cancer Research*, vol. 24, no. 21, pp. 5250–5260, Nov. 2018, doi:
710 10.1158/1078-0432.CCR-18-0309.
711 [62] S. Koyama *et al.*, "Adaptive resistance to therapeutic PD-1 blockade is associated with
712 upregulation of alternative immune checkpoints," *Nat Commun*, vol. 7, Feb. 2016,
713 doi: 10.1038/ncomms10501.
714 [63] M. R. Zaidi and G. Merlino, "The Two Faces of Interferon-γ in Cancer," *Clinical Cancer*
715 *Research*, vol. 17, no. 19, pp. 6118–6124, Oct. 2011, doi: 10.1158/1078-0432.CCR-11-
716 0482.
717 [64] R. D. Schreiber, L. J. Old, and M. J. Smyth, "Cancer Immunoediting: Integrating Im-
718 munity's Roles in Cancer Suppression and Promotion," 2011. [Online]. Available:
719 www.sciencemag.org
720 [65] B. Salomé *et al.*, "NKG2A and HLA-E define an alternative immune checkpoint axis in
721 bladder cancer," *Cancer Cell*, vol. 40, no. 9, pp. 1027-1043.e9, Sep. 2022, doi:
722 10.1016/j.ccell.2022.08.005.
723 [66] L. Borst, S. H. van der Burg, and T. van Hall, "The NKG2A–HLA-E Axis as a Novel
724 Checkpoint in the Tumor Microenvironment," *Clinical Cancer Research*, vol. 26, no.
725 21, pp. 5549–5556, Nov. 2020, doi: 10.1158/1078-0432.CCR-19-2095.
726 [67] M. Cui, J. Huang, S. Zhang, Q. Liu, Q. Liao, and X. Qiu, "Immunoglobulin Expression in
727 Cancer Cells and Its Critical Roles in Tumorigenesis," *Front Immunol*, vol. 12, Mar.
728 2021, doi: 10.3389/fimmu.2021.613530.
729 [68] X. Li *et al.*, "The Presence of IGHG1 in Human Pancreatic Carcinomas Is Associated
730 With Immune Evasion Mechanisms," *Pancreas*, vol. 40, no. 5, pp. 753–761, Jul. 2011,
731 doi: 10.1097/MPA.0b013e318213d51b.
732 [69] B. Pan, S. Zheng, C. Liu, and Y. Xu, "Suppression of IGHG1 gene expression by siRNA
733 leads to growth inhibition and apoptosis induction in human prostate cancer cell,"
734 *Mol Biol Rep*, vol. 40, no. 1, pp. 27–33, Jan. 2013, doi: 10.1007/s11033-012-1944-x.
735 [70] C. Qin *et al.*, "Cancer-driven IgG promotes the development of prostate cancer
736 though the SOX2-CIgG pathway," *Prostate*, vol. 80, no. 13, pp. 1134–1144, Sep. 2020,
737 doi: 10.1002/pros.24042.
738 [71] Z. Wang *et al.*, "Cancer-derived sialylated IgG promotes tumor immune escape by
739 binding to Siglecs on effector T cells," *Cell Mol Immunol*, vol. 17, no. 11, pp. 1148–
740 1162, Nov. 2020, doi: 10.1038/s41423-019-0327-9.
741 [72] H. Qin *et al.*, "Specific antitumor immune response induced by a novel DNA vaccine
742 composed of multiple CTL and T helper cell epitopes of prostate cancer associated
743 antigens," *Immunol Lett*, vol. 99, no. 1, pp. 85–93, Jun. 2005, doi:
744 10.1016/j.imlet.2005.01.006.

[73] W. K. Born, C. L. Reardon, and R. L. O'Brien, "The function of γδ T cells in innate immunity," *Current Opinion in Immunology*, vol. 18, no. 1. pp. 31–38, Feb. 2006. doi: 10.1016/j.coi.2005.11.007.
[74] F. Garrido, T. Cabrera, and N. Aptsiauri, "'Hard' and 'soft' lesions underlying the HLA class I alterations in cancer cells: Implications for immunotherapy," *International Journal of Cancer*, vol. 127, no. 2. pp. 249–256, Jul. 15, 2010. doi: 10.1002/ijc.25270.
[75] M. A. Garrido *et al.*, "Copy neutral loh affecting the entire chromosome 6 is a frequent mechanism of hla class i alterations in cancer," *Cancers (Basel)*, vol. 13, no. 20, Oct. 2021, doi: 10.3390/cancers13205046.
[76] K. van den Berge *et al.*, "RNA Sequencing Data: Hitchhiker's Guide to Expression Analysis," *Annu Rev Biomed Data Sci*, vol. 2, no. 1, pp. 139–173, Jul. 2019, doi: 10.1146/annurev-biodatasci-072018-021255.
[77] "cBioPortal for Cancer Genomics." https://www.cbioportal.org (accessed May 11, 2022).
[78] "GDC." https://portal.gdc.cancer.gov (accessed May 11, 2022).

Legends

Figure 1. MHC-I/-II high expression in CDK12 defective prostate cancer showed distinct transcriptome activity. (a) Transcriptome heatmap exhibiting clustering of top 50 DEGs in pPCa CDK12-Mut MHC-I High group (*n* = 30). The upper cluster (I) has IGHV and IGLV over-expressed genes linked to *CDK12* MHC I high. The central clusters (II and III) has four HLA genes overexpressed in the MHC I high group, supporting our CDK12 mutated MHC expression classification. The lower cluster (IV) has 14 downregulated genes when MHC I is highly expressed. **(b)** Transcriptome heatmap exhibiting clustering of top 50 DEGs in the pPCa CDK12-Mut MHC-II High group (*n* = 23). The upper cluster (I) has upregulation of genes related to cytotoxicity, immune cell migration, and immune suppression. We could not observe clinical features associated with MHC I or II clusters. **(c)** Transcriptome heatmap exhibiting clustering of top 50 DEGs in the mCRPC CDK12-Mut MHC High group (*n* = 6). The combined MHC I and II showed two distinct clusters. The lower cluster showed the upregulation of genes linked to innate and adaptative immune response and CD4+ and CD8+ T cell activity. **(d)** Enriched GO (BP) pathways of the upregulated genes from pPCa CDK12-

Mut MHC-I. **(e)** Enriched GO (BP) pathways of the upregulated genes from pPCa CDK12-Mut MHC-II High group. **(f)** Enriched GO (BP) pathways of the upregulated genes from the mCRPC CDK12-Mut High group. The DEGs are relative to the CDK12-Mut 'Low' group. Clinical information is displayed on top of the heatmap for each patient. The color scale in the heatmap represents the Z-score of the normalized read counts for each gene, where the red scale indicates upregulated and blue low-expressed genes. Enrichment analyses were performed using *clusterProfiler* and *p*-adjusted value = 0.05 as the cutoff. Bar plots show the top 20 most significant Gene Ontology (BP) terms.

Figure 2. MHC high expressed *CDK12* defective prostate tumors are associated with activation of immune-related pathways. (a) Gene Set Enrichment Analysis of Hallmark's pathways in pPCa *CDK12-Mut* MHC-I High (n = 30)**. (b)** Gene Set Enrichment Analysis of Hallmark pathways in pPCa *CDK12-Mut* MHC-II High (n = 23). **(c-d)** Gene Set Enrichment Analysis of Hallmarks and Reactome pathways in mCRPC *CDK12-Mut* MHC High (n = 10). A normalized enrichment score indicates each factor's positive or negative association with the condition of interest, which means activation or suppression of the pathway. Enrichment analyses were performed using *clusterProfiler* and *p*-adjusted value = 0.05 as the cutoff.

Figure 3. MHC high expressed CDK12 defective prostate cancer showed enhanced expression of immunomodulatory genes. RNA-sequencing expression level of immunomodulatory genes **(a)** *IDO1* ($p < 0.018$), **(b)** *HAVCR2* (*TIM3*) ($p < 0.0022$) in *CDK12-Mut* MHC-I High. n = 48; **(c)** *CD274* (*PD-L1*) ($p < 0.0028$), **(d)** *HAVCR2* (*TIM3*) ($p < 0.00012$), **(e)** *IDO1* ($p < 0.001$) in *CDK12-Mut* MHC-II High. n = 48; **(f)** *CD274* (*PD-L1*) ($p < 0.0095$). n = 10; *: *p*-value < 0.05; **: *p*-value < 0.01, by Mann-Whitney test. *IDO1*,

Indoleamine 2,3-Dioxygenase 1; *HAVCR3* (*TIM3*), T-Cell Immunoglobulin Mucin Receptor 3; *CD274* (*PD-L1*), Programmed Cell Death 1 Ligand 1.

Figure 4. MHC high expressed *CDK12* defective is associated with enhanced T cell recruitment of prostate tumors. (a) CIBERSORT-derived immune cell abundance of 22 distinct cell subsets based on *CDK12* defective MHC-I High pPCa (n = 30)**. (b)** CIBERSORT-derived immune cell abundance of 22 distinct cell subsets based on *CDK12* defective MHC-II High pPCa (n = 23). **(c)** CIBERSORT-derived immune cell abundance of 22 distinct cell subsets based on *CDK12* defective MHC High mCRPC (n = 10). *: p-value < 0.05; **: p-value < 0.01, by Mann-Whitney test.

Table 1. *CDK12* defective in primary MHC low expressed tumors. Integral results of FACETS analysis of whole-exome sequencing data from *CDK12* defective primary tumors expressing low levels of MHC-I/II. For each patient, the table shows the integer copy number for the allelic ratio of the heterozygous SNPs in the tumor/normal pair. The first column is the patient ID and the second column are the MHC region loci and other genes commonly subject to LOH in PCa. The last two columns represent the total copy number and the minor copy number, respectively. Tumors with a 2:1 ratio are considered normal for each position, while 2:0 and 1:0 represent CN-LOH and LOH events. The cellular fraction represents the estimated number of cells harboring the genotype. Primary PCa revealed subclonal CN-LOH and LOH at *JAK1, STAT1, IRF2, IRF1, MHC-I/II, TAP1, TAP2, IFNR1, JAK2, B2M, CIITA, NLRC5,* and *IFNR1*. Two patients showed biallelic loss at the *B2M* locus (Total copy number/minor copy number ratio=0:0). *MHC-I = *HLA-A, HLA-B,* and *HLA-C;* MHC-II = *HLA-DRA, HLA-DRB5, HLA-DRB6, HLA-DPA1, HLA-DPB1, HLA-DQA1, HLA-DQB1,* and *HLA-DQB2*.

Table 2. *CDK12* defective in metastatic MHC low expressed tumors. Integral results of FACETS analysis of whole-exome sequencing data from *CDK12* defective metastatic tumors expressing low levels of MHC-I/II. The same parameters shown in Table 1 were used to characterize LOH for each gene of interest. Metastatic PCa showed allele-specific copy number gains at *JAK1, STAT1, IRF2, IRF1, MHC-I/II, TAP1, TAP2, IFNR1, JAK2, B2M, CIITA, NLRC5,* and *IFNR1*. One patient showed a clonal LOH event at the *JAK2* and *B2M* loci (Total copy number/minor copy number ratio=1:0). *MHC-I = *HLA-A, HLA-B,* and *HLA-C;* MHC-II = *HLA-DRA, HLA-DRB5, HLA-DRB6, HLA-DPA1, HLA-DPB1, HLA-DQA1, HLA-DQB1,* and *HLA-DQB2*.

A

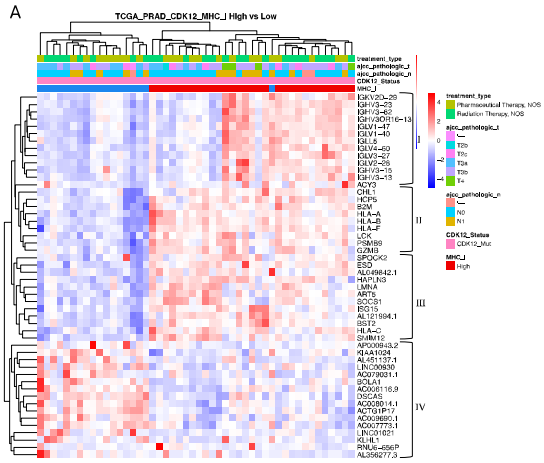

D

ID	Description	p.adjust
GO:0051249	regulation of lymphocyte activation	1,48E-19
GO:0002460	adaptive immune response based on somatic recombination of immune receptors built from immunoglobulin superfamily domains	1,48E-19
GO:0050867	positive regulation of cell activation	2,78E-20
GO:0002449	lymphocyte mediated immunity	1,16E-18
GO:0006958	complement activation, classical pathway	2,77E-14
GO:0006959	humoral immune response	1,08E-09
GO:0050853	B cell receptor signaling pathway	2,20E-08
GO:0002440	production of molecular mediator of immune response	7,15E-08
GO:0042742	defense response to bacterium	1,39E-07
GO:0006910	phagocytosis, recognition	5,66E-08

B

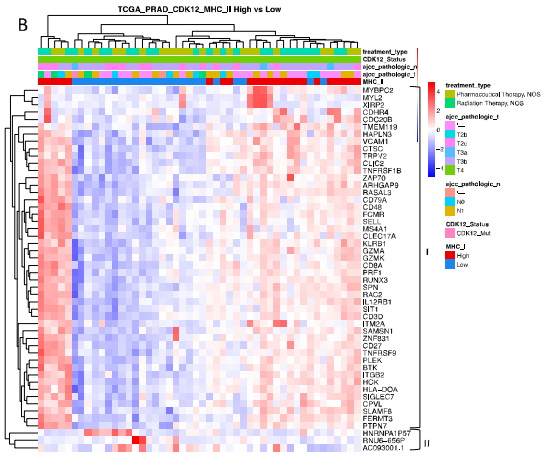

E

ID	Description	p.adjust
GO:0051249	regulation of lymphocyte activation	2,00E-25
GO:0042110	T cell activation	5,84E-25
GO:0050867	positive regulation of cell activation	9,60E-23
GO:0007159	leukocyte cell-cell adhesion	2,50E-20
GO:0002460	adaptive immune response based on somatic recombination of immune receptors built from immunoglobulin superfamily domains	2,80E-20
GO:0002443	leukocyte mediated immunity	3,53E-19
GO:1903037	regulation of leukocyte cell-cell adhesion	8,17E-19
GO:0070661	leukocyte proliferation	1,75E-15
GO:0046651	lymphocyte proliferation	5,77E-14
GO:0070663	regulation of leukocyte proliferation	1,64E-12

C

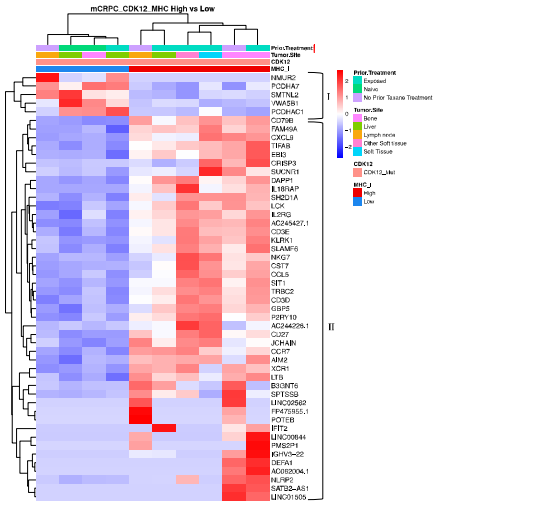

F

ID	Description	p.adjust
GO:0051251	positive regulation of lymphocyte activation	4,87E-15
GO:0002449	lymphocyte mediated immunity	6,43E-15
GO:0002253	activation of immune response	6,67E-15
GO:0042110	T cell activation	3,27E-11
GO:0002460	adaptive immune response based on somatic recombination of immune receptors built from immunoglobulin superfamily domains	1,76E-09
GO:0006959	humoral immune response	1,21E-06
GO:0019724	B cell mediated immunity	2,55E-06
GO:0050863	regulation of T cell activation	9,19E-07
GO:0007159	leukocyte cell-cell adhesion	3,27E-04
GO:1903037	regulation of leukocyte cell-cell adhesion	1,75E-03

Figure 1

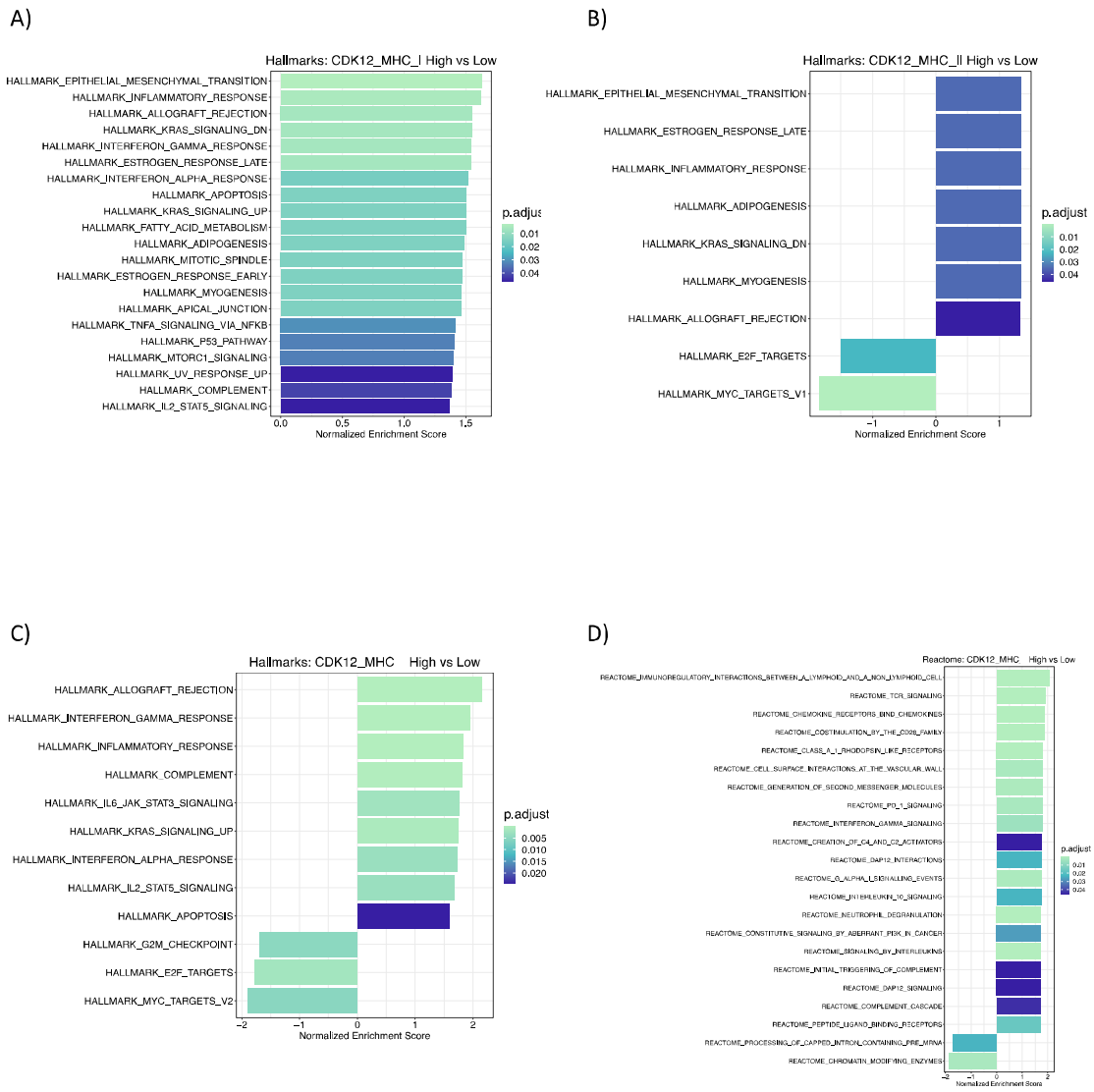
A)
Hallmarks: CDK12_MHC_I High vs Low
HALLMARK_EPITHELIAL_MESENCHYMAL_TRANSITION
HALLMARK_INFLAMMATORY_RESPONSE
HALLMARK_ALLOGRAFT_REJECTION
HALLMARK_KRAS_SIGNALING_DN
HALLMARK_INTERFERON_GAMMA_RESPONSE
HALLMARK_ESTROGEN_RESPONSE_LATE
HALLMARK_INTERFERON_ALPHA_RESPONSE
HALLMARK_APOPTOSIS
HALLMARK_KRAS_SIGNALING_UP
HALLMARK_FATTY_ACID_METABOLISM
HALLMARK_ADIPOGENESIS
HALLMARK_MITOTIC_SPINDLE
HALLMARK_ESTROGEN_RESPONSE_EARLY
HALLMARK_MYOGENESIS
HALLMARK_APICAL_JUNCTION
HALLMARK_TNFA_SIGNALING_VIA_NFKB
HALLMARK_P53_PATHWAY
HALLMARK_MTORC1_SIGNALING
HALLMARK_UV_RESPONSE_UP
HALLMARK_COMPLEMENT
HALLMARK_IL2_STAT5_SIGNALING
0.0
0.5
1.0
1.5
Normalized Enrichment Score
p.adjus
0.01
0.02
0.03
0.04
B)
Hallmarks: CDK12_MHC_II High vs Low
HALLMARK_EPITHELIAL_MESENCHYMAL_TRANSITION
HALLMARK_ESTROGEN_RESPONSE_LATE
HALLMARK_INFLAMMATORY_RESPONSE
HALLMARK_ADIPOGENESIS
HALLMARK_KRAS_SIGNALING_DN
HALLMARK_MYOGENESIS
HALLMARK_ALLOGRAFT_REJECTION
HALLMARK_E2F_TARGETS
HALLMARK_MYC_TARGETS_V1
−1
0
1
Normalized Enrichment Score
p.adjust
0.01
0.02
0.03
0.04
C)
Hallmarks: CDK12_MHC High vs Low
HALLMARK_ALLOGRAFT_REJECTION
HALLMARK_INTERFERON_GAMMA_RESPONSE
HALLMARK_INFLAMMATORY_RESPONSE
HALLMARK_COMPLEMENT
HALLMARK_IL6_JAK_STAT3_SIGNALING
HALLMARK_KRAS_SIGNALING_UP
HALLMARK_INTERFERON_ALPHA_RESPONSE
HALLMARK_IL2_STAT5_SIGNALING
HALLMARK_APOPTOSIS
HALLMARK_G2M_CHECKPOINT
HALLMARK_E2F_TARGETS
HALLMARK_MYC_TARGETS_V2
−2
−1
0
1
2
Normalized Enrichment Score
p.adjust
0.005
0.010
0.015
0.020
D)
Reactome: CDK12_MHC High vs Low
REACTOME_IMMUNOREGULATORY_INTERACTIONS_BETWEEN_A_LYMPHOID_AND_A_NON_LYMPHOID_CELL
REACTOME_TCR_SIGNALING
REACTOME_CHEMOKINE_RECEPTORS_BIND_CHEMOKINES
REACTOME_COSTIMULATION_BY_THE_CD28_FAMILY
REACTOME_CLASS_A/1_(RHODOPSIN_LIKE_RECEPTORS)
REACTOME_CELL_SURFACE_INTERACTIONS_AT_THE_VASCULAR_WALL
REACTOME_GENERATION_OF_SECOND_MESSENGER_MOLECULES
REACTOME_PD_1_SIGNALING
REACTOME_INTERFERON_GAMMA_SIGNALING
REACTOME_CREATION_OF_C4_AND_C2_ACTIVATORS
REACTOME_DAP12_INTERACTIONS
REACTOME_G_ALPHA_(S)_SIGNALLING_EVENTS
REACTOME_INTERLEUKIN_10_SIGNALING
REACTOME_NEUTROPHIL_DEGRANULATION
REACTOME_CONSTITUTIVE_SIGNALING_BY_ABERRANT_PI3K_IN_CANCER
REACTOME_SIGNALING_BY_INTERLEUKINS
REACTOME_INITIAL_TRIGGERING_OF_COMPLEMENT
REACTOME_DAP12_SIGNALING
REACTOME_COMPLEMENT_CASCADE
REACTOME_PEPTIDE_LIGAND_BINDING_RECEPTORS
REACTOME_PROCESSING_OF_CAPPED_INTRON_CONTAINING_PRE_MRNA
REACTOME_CHROMATIN_MODIFYING_ENZYMES
−2
−1
0
1
2
Normalized Enrichment Score
p.adjust
0.21
0.22
0.23
0.24

Figu

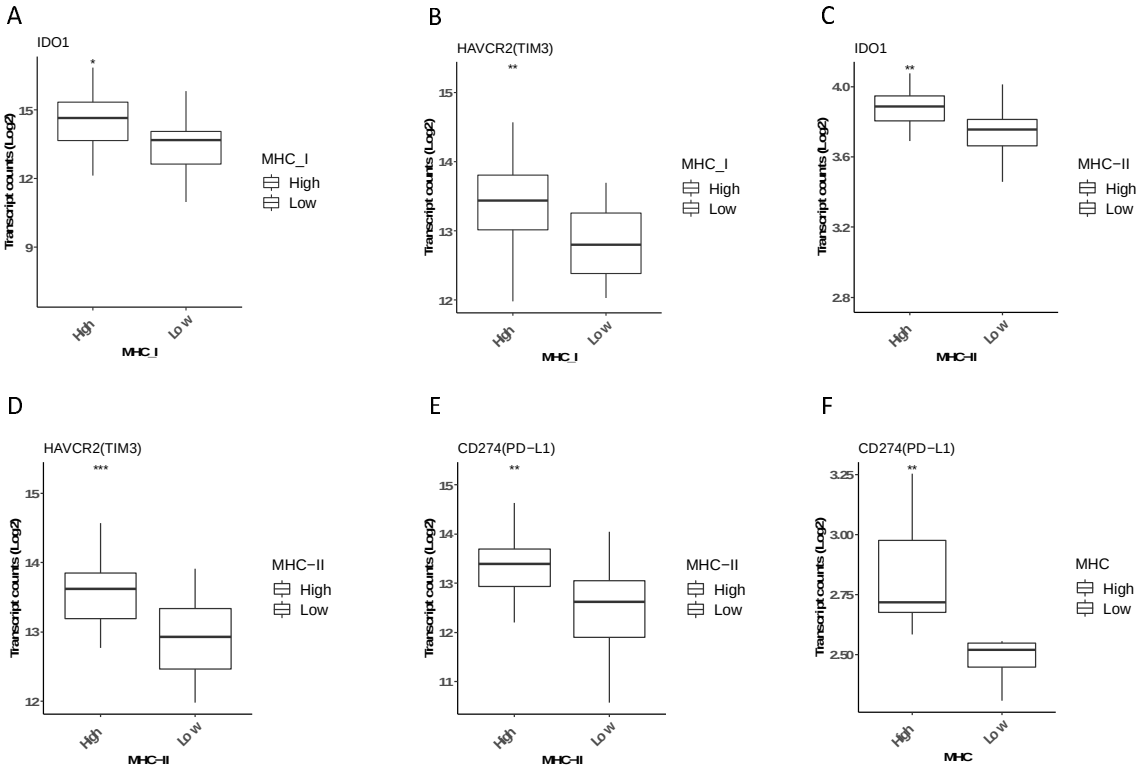
A
IDO1
Transcript counts (Log2)
MHC_I
High
Low
B
HAVCR2(TIM3)
C
IDO1
MHC−II
D
HAVCR2(TIM3)
E
CD274(PD−L1)
F
CD274(PD−L1)
MHC

Figure 3

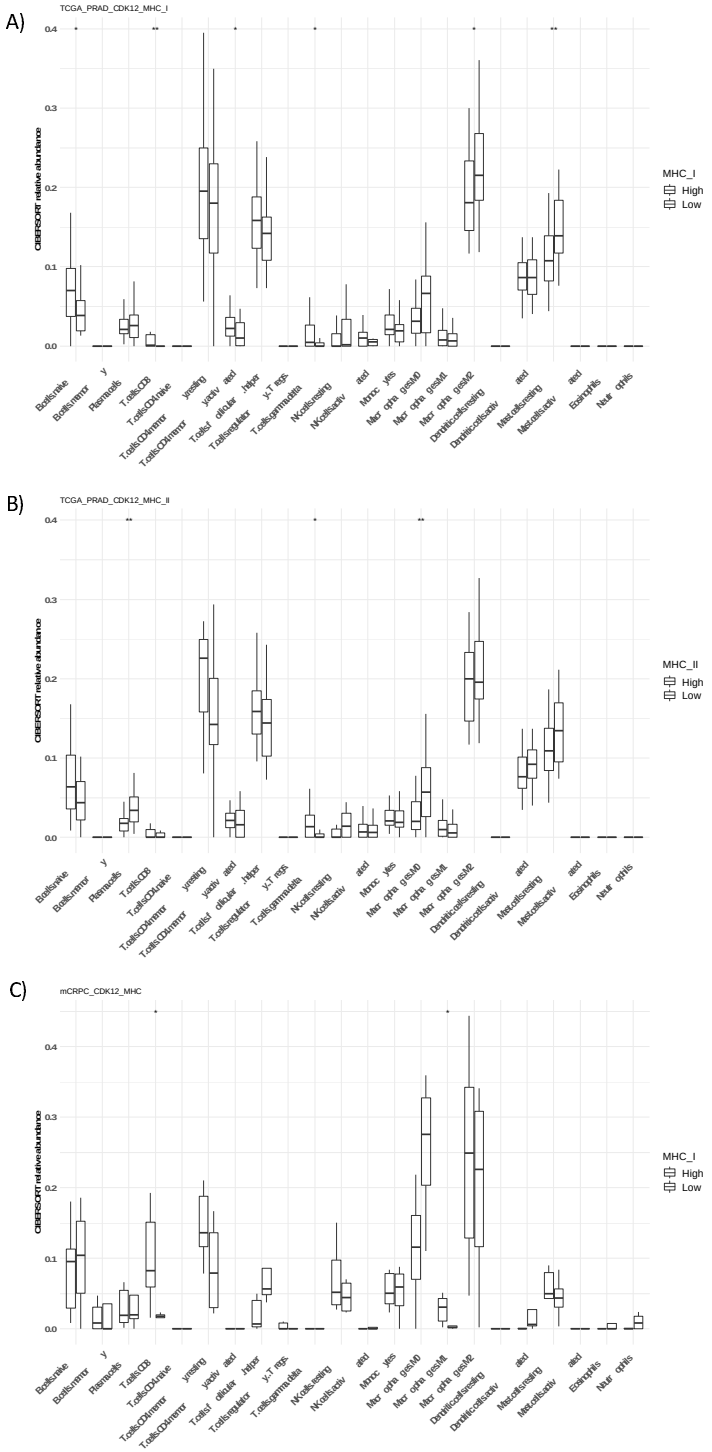
A)
TCGA_PRAD_CDK12_MHC_I
CIBERSORT relative abundance
MHC_I
High
Low
B)
TCGA_PRAD_CDK12_MHC_II
CIBERSORT relative abundance
MHC_II
High
Low
C)
mCRPC_CDK12_MHC
CIBERSORT relative abundance
MHC_I
High
Low

Figure 4

Patient ID	Gene	chrom	start	end	cellular fraction	Total copy number	Minor copy number
TCGA-KK-A8IA	*STAT1*	2	134713128	192194260	0.833	1	0
TCGA-KK-A8IA	*IRF1*	5	55231421	143147410	0.833	1	0
TCGA-KK-A8IA	*PTEN*	10	87552401	89139399	0.833	1	0
TCGA-KK-A8IA	*B2M*	15	41191425	77615398	0.208	0	0
TCGA-KK-A8IG	*IFNGR1*	6	65302925	170584366	0.668	1	0
TCGA-KK-A8I6	*PTEN*	10	73243437	104454566	0.332	0	0
TCGA-KK-A8I6	*NLRC5*	16	49396608	90096324	0.11	0	0
TCGA-XJ-A9DX	*NLRC5*	16	49280867	57722991	0.62	1	0
TCGA-ZG-A9LM	*STAT1*	2	134317491	192057773	0.47	2	0
TCGA-ZG-A9LM	*B2M*	15	19882284	101922415	0.47	2	0
TCGA-ZG-A9LM	*NLRC5*	16	56276055	89228602	0.47	2	0
TCGA-EJ-8472	*JAK1*	1	21619903	67705610	0.37	1	0
TCGA-EJ-8472	*B2M*	15	42751857	97971259	0.37	2	0
TCGA-XQ-A8TA	*IRF2*	4	177976002	189984351	0.92	1	0
TCGA-XQ-A8TA	*IRF1*	5	128464930	181260211	0.92	2	0
TCGA-XQ-A8TA	*PTEN*	10	87790275	89599433	0.92	0	0
TCGA-YL-A8HO	*STAT1*	2	119157673	199659594	0.12	0	0
TCGA-YL-A8HO	*IRF1*	5	143082	181260211	0.38	2	0
TCGA-YL-A8HO	*MHC-I/II, *TAP1/2*	6	304637	170584276	0.27	1	0
TCGA-YL-A8HO	*IFNGR1*	6	304637	170584276	0.27	1	0
TCGA-YL-A8HO	*B2M*	15	19882294	101922415	0.27	1	0
TCGA-YL-A8HO	*CIITA*	16	8644541	58196892	0.22	2	0
TCGA-YL-A8HO	*NLRC5*	16	8644541	58196892	0.22	2	0
TCGA-XK-AAJA	*PTEN*	10	7243639	12235132	0.54	1	0
TCGA-KK-A7AP	*B2M*	15	33311111	57091863	0.87	1	0
TCGA-KK-A7AP	*NLRC5*	16	48347484	90177833	0.87	1	0
TCGA-HC-7744	*B2M*	15	42515191	45178103	0.12	0	0
TCGA-KK-A8IG	*IFNGR1*	6	65302925	170584366	0.668	1	0
TCGA-EJ-7784	*JAK2*	9	14859	18718116	0.437	1	0
TCGA-HC-A48F	*JAK1*	1	41513578	80451865	0.86	1	0
TCGA-HC-A48F	*IRF2*	4	85671	189984257	0.21	1	0
TCGA-HC-A48F	*IRF1*	5	54400082	171456817	0.86	1	0
TCGA-HC-A48F	*MHC-I/II, *TAP1/2*	6	304637	170584366	0.31	1	0
TCGA-HC-A48F	*IFNGR1*	6	304637	170584366	0.31	1	0
TCGA-HC-A48F	*PTEN*	10	49168049	118015066	0.21	1	0
TCGA-HC-A48F	*B2M*	15	44380814	50749712	0.86	1	0
TCGA-HC-A48F	*NLRC5*	16	35085998	90177833	0.86	1	0

Table1

Patient ID	Gene	chrom	start	end	cellular fraction	Total copy number	Minor copy number
5115412	*JAK1*	1	33804897	68440771	0.49	5	2
5115412	*STAT1*	2	187346385	205615949	0.54	5	2
5115412	*IRF2*	4	182891198	185757023	0.87	6	2
5115412	*IRF1*	5	112892242	139881181	0.81	4	2
5115412	MHC-I	6	29555893	32256053	0.87	4	1
5115412	MHC-II	6	32288409	38345160	0.30	6	2
5115412	*TAP-1*	6	32288409	38345160	0.30	6	2
5115412	*TAP-2*	6	32288409	38345160	0.30	6	2
5115412	*JAK2*	9	2804198	15486990	0.59	4	2
5115412	*PTEN*	10	80253502	93958843	0.30	6	2
5115412	*B2M*	15	30626570	59138344	0.59	4	2
5115412	*CIITA*	16	198972	17358048	0.59	4	2
5115412	*NLRC5*	16	57372390	71634040	0.52	4	2
5115412	*IFNGR2*	21	33230307	34889712	0.87	5	2
1115161	*IRF2*	4	184116877	186709443	0.51	6	3
1115161	*HLA-A*	6	29330997	30628358	0.79	3	1
1115161	*HLA-B*	6	30635016	31382266	0.59	5	2
1115161	*HLA-C*	6	30635016	31382266	0.59	5	2
1115161	*JAK2*	9	52538	33113788	0.20	3	1
5115615	*JAK1*	1	63571201	65432064	0.912	3	1
5115615	*STAT1*	2	188522965	192194738	0.912	3	1
5115615	MHC-I	6	29944749	30415099	0.899	3	1
5115615	MHC-I/II	6	30469283	32407241	0.902	4	2
5115615	MHC-II	6	32439760	32666486	0.912	3	1
5115615	MHC-II/*TAP1/2*	6	32666737	34289022	0.902	4	2
5115615	*JAK2*	9	117666	9091026	0.906	1	0
5115615	*B2M*	15	41691484	46828068	0.906	1	0
5115615	*CIITA*	16	9938304	11178578	0.912	3	1
5115615	*IFNGR2*	21	33335636	37018290	0.899	3	1

Table 2